UNIVERSIDADE FEDERAL DO RIO GRANDE DO SUL

ESCOLA DE ENGENHARIA - CURSO DE ENGENHARIA MECÂNICA

TRABALHO DE CONCLUSÃO DE CURSO

PROCESS OPTIMIZATION OF REFILL FRICTION STIR SPOT WELDING OF CAST
ALUMINUM (AlSi10) TO AlSi-COATED PRESS HARDENED STEEL (PHS1500AlSi)

por

Rafael Maltz Piccoli

Monografia apresentada ao Departamento de Engenharia Mecânica da Escola de Engenharia da Universidade Federal do Rio Grande do Sul, como parte dos requisitos para obtenção do diploma de Engenheiro Mecânico.

Porto Alegre, Fevereiro de 2024.

CIP - Catalogação na Publicação

Rafael Maltz Piccoli

PROCESS OPTIMIZATION OF REFILL FRICTION STIR SPOT WELDING OF CAST ALUMINUM (AlSi10) TO AlSi-COATED PRESS HARDENED STEEL (PHS1500AlSi)

ESTA MONOGRAFIA FOI JULGADA ADEQUADA COMO PARTE DOS REQUISITOS PARA A OBTENÇÃO DO TÍTULO DE

ENGENHEIRO MECÂNICO

APROVADA EM SUA FORMA FINAL PELA BANCA EXAMINADORA DO CURSO DE ENGENHARIA MECÂNICA

Prof. Dr. Ignácio Iturrioz
Coordenador do Curso de Engenharia Mecânica

Área de concentração: **Processos de Fabricação**

Orientadora: Profª. Dra. Cíntia Cristiane Petry Mazzaferro

Comissão de Avaliação:

Profa. Dra. Cíntia Cristiane Petry Mazzaferro (Presidente)

Prof. Dr. Arnaldo Ruben Gonzalez

Prof. Dr. Jakson Manfredini Vassoler

Prof. Dr. Patric Daniel Neis

Porto Alegre, Fevereiro de 2024.

DEDICATÓRIA

Dedico este trabalho de diplomação à minha família e principalmente à minha mãe, Renata Maltz. O apoio incondicional foi a chave que tornou possível o rumo dessa jornada. Montanhas foram movidas para que eu pudesse realizar o sonho de me fornar Engenheiro Mecânico. Pessoas exemplares que sempre prezaram pelos meus estudos e que me motivaram a nunca desistir.

AGRADECIMENTOS

Agradeço à Universidade Federal do Rio Grande do Sul por oferecer um ensino de excelência de forma gratuita. Aos professores que dedicaram seu tempo e conhecimento à formar, não apenas um engenheiro, mas uma pessoa melhor e apaixonada pela profissão.

À minha família, que foi meu pilar fundamental de apoio e inesgotável inspiração.

À minha amada namorada Júlia Martins por todo apoio, inclusive nos momentos mais frustrantes do fim do curso.

Aos meus melhores amigos pelas parcerias e inúmeras aventuras que tive o prazer de compartilhar. Em especial ao Daniel Smejoff, Júlia Scheir, Vinicius Machado e Felipe Grossi pelo companheirismo ao longo de décadas de amizade.

Ao Exército Brasileiro pela formação de Oficial Combatente pelo Centro de Preparação de Oficiais da Reserva (CPOR/PA), onde pude me desenvolver profissionalmente e pessoalmente logo no primeiro ano da faculdade.

Aos colegas do Laboratório de Metalurgia Física (LAMEF) por terem me proporcionado a oportunidade de iniciar minha carreira profissional durante os cinco anos de Iniciação Científica, principalmente ao Fabiano Mattei e Marcelo Favaro pelo voto de confiança.

Aos colegas do Centro de Pesquisa Helmholtz-Zentrum Hereon em Geesthacht, Alemanha, que convivi dioturnamente durante um ano de estágio e pela possibilidade de realizar o presente trabalho com equipamentos de ponta e supervisão de pessoas extremamente talentosas e profissionais.

À Stresstec Engenharia pelo período de estágio obrigatório e valiosos ensinamentos que uma empresa séria possui.

À orientadora Prof. Cíntia Mazzaferro, por toda atenção e disponibilidade ao transmitir a vasta sabedoria e experiência no assunto sobre soldagem por fricção para que este trabalho fosse concluído.

Conhecer a si mesmo é o começo de toda sabedoria.

Aldous Huxley

Piccoli, Rafael Maltz. **Otimização do Processo de Soldagem a Ponto por Fricção Entre Alumínio Fundido (AlSi10) e Aço Endurecido por Conformação com Revestimento de AlSi (PHS1500AlSi).** 2024. 30 páginas. Monografia de Trabalho de Conclusão de Curso em Engenharia Mecânica – Curso de Engenharia Mecânica, Universidade Federal do Rio Grande do Sul, Porto Alegre, 2024.

RESUMO

O presente trabalho estudou a otimização do processo de soldagem a ponto por fricção (RFSSW) para o resultado do teste de resistência ao cisalhamento entre placas de alumínio fundido (AlSi10) com 3,0 mm de espessura e placas de aço endurecido por conformação (PHS1500AlSi) com 1,4 mm de espessura na configuração de sobreposição. Durante a etapa de testes preliminares, foi analisada a viabilidade de soldagem para três condições de superfície diferentes do aço, em relação à presença de revestimento. Para a condição de superfície original (revestimento eutético de AlSi) foi demonstrada a impossibilidade de soldagem. Para a condição de superfície intermediária (revestimento intermetálico de Al_7Fe_2Si) e para a condição de superfície exposta do aço (sem revestimento) foi possível obter a união metalúrgica. Deste modo, foi determinada a janela de combinação de parâmetros de soldagem (velocidade de rotação, velocidade de penetração/recuo e tempo de mistura) que resultou em soldas sem defeitos. Além disso, a superfície exposta do aço foi a melhor opção para continuar com a otimização dos parâmetros do processo, tendo em vista o desempenho mecânico. O planejamento experimental Box-Behnken, através de superfícies de resposta, e o software de análise estatística Minitab, através da análise de variância, foram utilizados para auxiliar na otimização da combinação dos parâmetros de soldagem que resultaram na máxima resistência ao cisalhamento das juntas e, ao mesmo tempo, com mínimo desvio-padrão. Por fim, a significância estatística e a influência de cada parâmetro na resposta do teste de cisalhamento puderam ser avaliadas graficamente e com base na equação de regressão.

PALAVRAS-CHAVE: Otimização de Parâmetros, Box-Behnken, RFSSW, AlSi10, PHS1500AlSi.

Piccoli, Rafael Maltz. **Process Optimization of Refill Friction Stir Spot Welding of Cast Aluminum (AlSi10) to AlSi-Coated Press Hardened Steel (PHS1500).** 2024. 30 pages. Monography for Bachelor Degree of Mechanical Engineering – Mechanical Engineering Course, The Federal University of Rio Grande do Sul, Porto Alegre, 2024.

ABSTRACT

The present work studied the process optimization of refill friction stir spot welding (RFSSW) for the response of lap shear strength (LSS) between cast aluminum (AlSi10) 3.0 mm thick plates and press hardened steel (PHS1500AlSi) 1.4 mm thick plates in the configuration of overlapped sheets. During the preliminary testing stage, the feasibility of welding dissimilar materials was analyzed for three different surface conditions of the steel, in relation to the presence of coating. For the original surface condition (eutectic AlSi-coating) the impossibility of bonding was demonstrated. For the intermediate surface condition (Al_7Fe_2Si intermetallic coating) and for the exposed steel surface condition (uncoated) it was possible to obtain the metallurgical bond. Based on that, the process parameters combination window (rotation speed, plunge speed and dwell time) that would result in defect-free welds was datermined. Furthermore, the exposed surface of the steel was the best option to continue the process parameters optimization. Box-Behnken design of experiments, through response of surfaces, and Minitab statistical software, through analysis of variance, were used to optimize the combination of welding parameters that resulted in maximized LSS of the joints with minimum standard deviation. Finnaly, the statistical significance and influence of each parameter on the shear test response could be evaluated graphically and based on the regression equation in uncoded units.

KEYWORDS: Process Parameters Optimization, Box-Behnken, RFSSW, AlSi10, PHS1500AlSi.

LISTA DE ABREVIATURAS E SIGLAS

AHSS	Advanced High Strength Steel
ANOVA	Analysis of Variance
BBD	Box-Behnken Design
BM	Base Material
CF	Clamping Force
DOE	Design of Experiment
DP	Dual Phase
DT	Dwell Time
EU-RFCS	European Union Research Fund for Coal and Steel
FW	Friction Welding
FSW	Friction Stir Welding
FSSW	Friction Stir Spot Welding
HAZ	Heat Affected Zone
HF	Hot Formed
HI	Heat Input
IMC	Intermetallic Compound
ISO	International Standard Organization
LSS	Lap Shear Strength (Ultimate)
MS	Martensite
OFAT	One Factor at Time
PD	Plunge Depth
PHS	Press Hardened Steel
PS	Plunge Speed
RS	Rotational Speed
RSM	Response Surface Methodology
RFSSW	Refill Friction Stir Spot Welding
SZ	Stirred Zone
TMAZ	Thermomechanical Affected Zone
TWI	The Welding Institute
TF	Travel Factor
TRIP	Transformation Induced Plasticity
UHSS	Ultra High Strength Steel
WSA	World Steel Association

LISTA DE FIGURAS

SUMÁRIO

1. INTRODUCTION

The automotive industry has always been driven by the need to innovate. Fierce competition, high quality standards and environmental legislation force manufacturers to develop new materials and technologies capable to reach this need. The European Union Research Fund for Coal and Steel (EU-RFCS) aims for reducing automotive emissions by 30 % to 40 % until 2030, which is mainly achieved by lightweighting components, increasing fuel efficiency and electrification approaches [Stir4Steel Project, 2021].

Relatively new materials such as advanced high strength steels (AHSS) and press hardened steels (PHS) can promote considerable weight constrictions by downgauging, or using thinner sheets, because of their high strength-to-weight ratio [Costa, 2006]. Another material undergoing of constant improvement are the aluminum (Al), wrought and die cast, which also have an excellent alliance between mechanical properties and low weight [Hartlieb, 2013]. Definitely, PHS combined with cast Al could be able to provide this innovation for automotive industry and is already being considered as an alternative solution for the production of shock tower components, as shown in Figure 1.
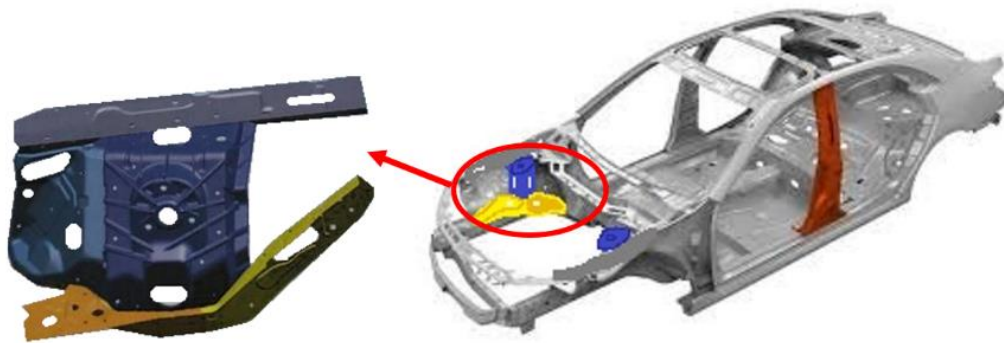
Figure 1 – Illustrative figure of a shock tower from an automotive structural component.
Source: adaptation from Stir4Steel Project (2021).

However, hybrid structures have always been a challenge to be produced due to the differences in physical and metallurgical properties between steel and aluminum. Riveting is traditionally used for this application, but it adds weight to the body. Fusion welding methods, as resistance and arc welding, becomes unfeasible due to substantial differences in melting point and thermal expansion, becoming susceptible to cracking during solidification [Mitra, 2001]. The high levels of heat input (HI) by the fusion of these materials also favors the intense formation of brittle intermetallic compounds (IMC) due to the low solubility of iron (Fe) in the Al matrix, thus degrading the mechanical properties of the joint [Fisher, 2015].

Refill friction stir spot welding (RFSSW) is a solid-state joining process developed by researchers at Helmholz-Zentrum Hereon in Germany. This technology is suitable for spot joining lightweight low melting point materials such as aluminum alloys in similar and dissimilar combination [Suhuddin, 2013]. This innovative way of fastening could join a variety of alloys that were not consider or even possible to weld. The advantages, such as no weight addiction, no requirement of consumables, flux or shielding gas, lower heat input, less energy consumption and compatibility of joining dissimilar materials, make RFSSW considered a promising alternative to riveting and fusion-based welding processes [Shen, 2022].

2. OBJECTIVES

The present work aims to study the process parameters optimization of RFSSW between cast aluminum (AlSi10) 3.0 mm thick plates and AlSi-coated press hardened steel (PHS1500AlSi) 1.4 mm thick plates in the configuration of overlapped sheets.

The specific objectives of this work are:

a) Find the parameter combination window that would result in defect-free welds;

b) Optimize the welding process parameters combination in order to maximize the lap shear strength (LSS) of the joints with minimized standard deviation;

c) Evaluate the influence of each parameter for the LSS test response.

3. LITERATURE REVIEW

3.1 BASE MATERIALS FOR AUTOMOTIVE INDUSTRY

The automotive industry has a large number of requirements regarding the material's behavior and reliability. Catering to vehicle components safety and fuel efficiency, the structural service condition is diverse. Traditionally in the manufacture of automobiles, the approximately proportion in equivalent weight for metal alloys are steel (60 %), aluminum (15 %) and magnesium (up to 5 %), while plastic and polymers (20 %) [World Steel Association].

Advanced high strength steels (AHSS) are a relatively new group of chemically controlled and mechanically enhanced steel grades (from 500 MPa). For example, dual phase (DP), transformation induced plasticity (TRIP) and hot-formed (HF) steels provide high-energy absorption during impacts. The ultra-high strength steels (UHSS) are a subgroup of the more comprehensive category of AHSS, with significantly higher ultimate tensile strength (from 800 MPa to 2 GPa). For this context, press hardened steel (PHS) provides strength without sacrificing formability, aiding in lightweighting for fuel efficiency. Additionally, Martensitic steels (MS) offers improved crash performance, suitable for anti-intrusion parts, due to the high levels of stiffness [World Steel Association]. These materials can be combined for optimal properties in specific areas of the car's body. The cladding behavior is also important for corrosion or abrasive protection, as zinc galvanization or AlSi-coating, respectively.

Aluminum alloys, as wrought and die cast, are overcoming in the automotive industry. These alloys are 30 % to 40 % lighter than steel, therefore it allows to reduce the fuel consumption as well. It is a mechanically resistant material with good energy absorption capacity combined with corrosion passivity [Hartlieb, 2013].

3.1.1. AlSi-Coated Press Hardened Steel 1500 MPa (PHS1500AlSi)

Press hardened steels are intended for use in automotive structural and safety components and its martensitic microstructure and properties are obtained by the quenching during conformation. The many advantages include the ability to obtain complex geometries, due to austenitic condition inside the stamping process, low levels of springback, uniformity of mechanical properties, impact resistance and noted fatigue strength. The AlSi-coating has excellent resistance to perforation corrosion, currently used in dry and wet areas of the vehicle. This cladding layer, applied at quenching course, still simplifies the process eliminating the protective oil shot blasting after stamping [ArcelorMittal].

3.1.2. Die Cast Aluminum (AlSi10)

The cast Al-Si-Mg alloys are defined as AA-3XX series and the Si content of 10 % constitutes a hypoeutectic solution. This material combines great strength-to-weight ratio and the differential advantage of this alloy is the excellent castability, from large structural components until thin objects, because of the lower melting point. In addition, good machinability and mechanical properties boosts a wide range of applications including the aerospace and automotive industries [Shakil, 2021].

3.2. FRICTION WELDING (FW)

Friction welding is a solid-state joining process, instead of the traditional fusion-based process. The metallurgical bonding occurs due to mechanical mixing and partial diffusion on the softened region. The relative motion between surfaces generates heat through mechanical friction, as illustrated in Figure 2. The first applications and patents regarding this method date back to 20's century for rotatory flywheel friction welding [Wang, 1974].
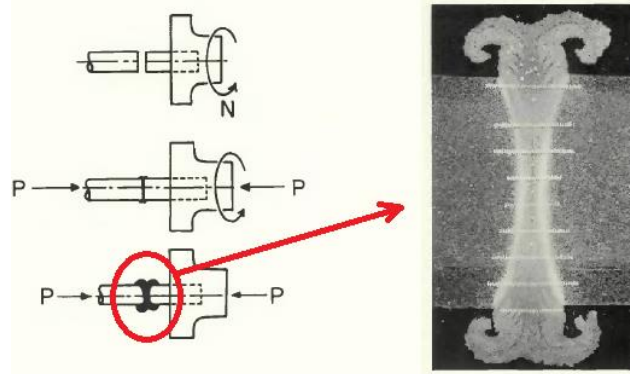
Figure 2 – Schematic illustration of flywheel friction welding process. Source: adapted from Wang et al. (1974).

3.2.1. Friction Stir Welding (FSW)

Friction stir welding (FSW) is a joining process that uses a non-consumable tool to join two facing workpieces, as linear butt welding, without reaching the melting point. The rotatory tool leads to a softened region, called stir zone, which mechanically intermixes the two pieces of metal, as shown in Figure 3. This friction-based process has the capability to weld a range of alloys, similar and dissimilar, that were considered impractical or even impossible to join using previous methods [Fisher, 2015]. FSW was invented and patented by Wayne Thomas at The Welding Institute (TWI), United Kingdom, in 1991 [Thomas, 1991].

Figure 3 – Schematic illustration of conventional FSW process. Source: adapted from Nandan et al. (2008).

3.2.2. Friction Stir Spot Welding (FSSW)

Friction stir spot welding (FSSW) is one of the many variations of the FSW process. The main difference is the welding configuration and the movement of the tool. A singular spot weld in lap configuration replaces the linear FSW in butt joints geometry. The FSSW process occurs over three stages: plunging, stirring, and retracting the rotatory tool, as shown in Figure 4. As a result, from the tool's profile, an exit hole is left inside the stirred zone (SZ), which causes high-stress concentrations in the joint [Yang, 2014.]
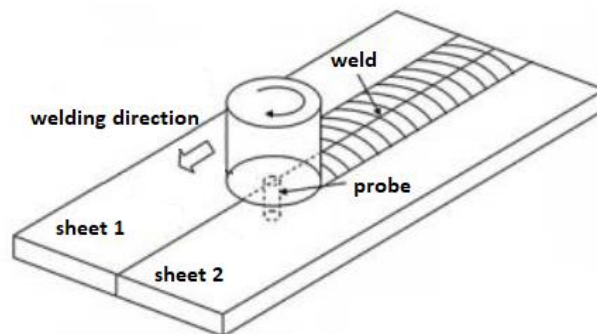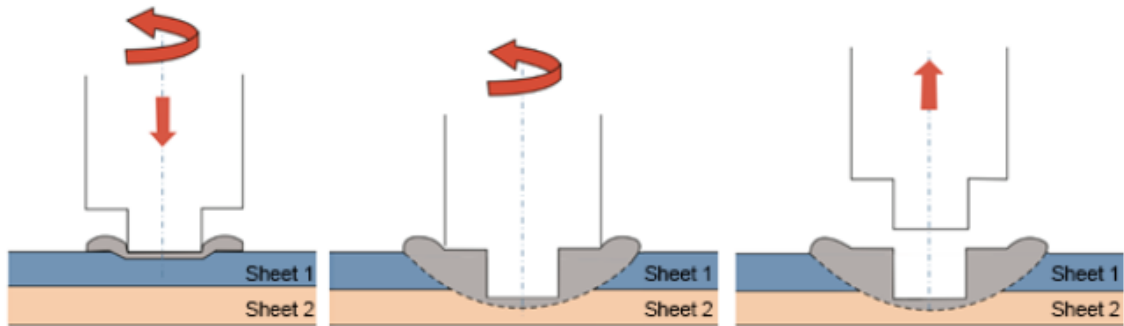
Figure 4 – f Schematic illustration of conventional FSSW process. Source: adapted from Yang et al. (2014).

3.2.3. Refill Friction Stir Spot Welding (RFSSW)

Refill friction stir spot welding (RFSSW) is an alternative presented to overcome the exit hole from FSSW. This friction-based process developed by researchers at Helmholz-Zentrum Hereon, in 1999, is suitable for spot welding lightweight materials in lap configuration achieving flat surface with minimal material loss [dos Santos, 1999.].

According to the standard ISO 18785:2018, two operating modes are possible. Probe or shoulder plunge modes are related in which element of the tool set penetrates on the top sheet. The clamping ring fix the plates against a backing plate and avoid flash formation. The shoulder plunge mode consists in four stages, as schematically illustrated in Figure 5.
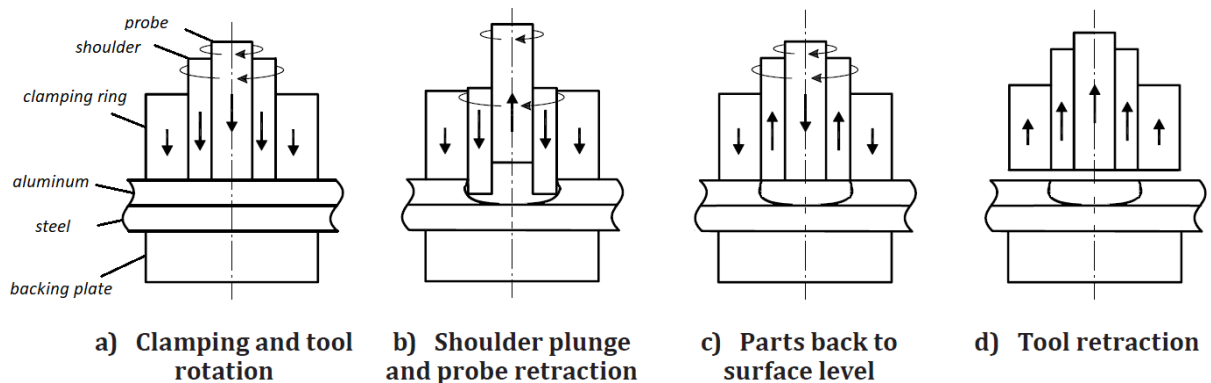
Figure 5 – Schematic illustration of shoulder plunge mode of RFSSW process. Source: adapted from ISO 18785:2018.

The workpiece material experiences a substantial change in the microstructure due to the frictional heat and the plastic deformation resulting from the tool spindle. Primarily, the microstructure of a RFSSW can be distinguished into three zones: stirred zone (SZ), thermo-mechanically affected zone (TMAZ) and heat-affected zone (HAZ) beyond the base material (BM), as shown in Figure 6.

The material in the SZ has direct contact with the rotating tool and suffer with the highest temperature and shear rate during the welding process. Dynamic recrystallization usually can be observed in the equiaxial and refined grain zone [Zou, 2021. Cao, 2016]. The narrow region close to the plunged shoulder is the TMAZ, which experiences the high temperatures from the SZ and the plastic deformation. These effects are not enough to provide dynamic recrystallization. The HAZ has no plastic deformation and its mechanical properties are only affected by the welding thermal cycle [Santos, 2020].
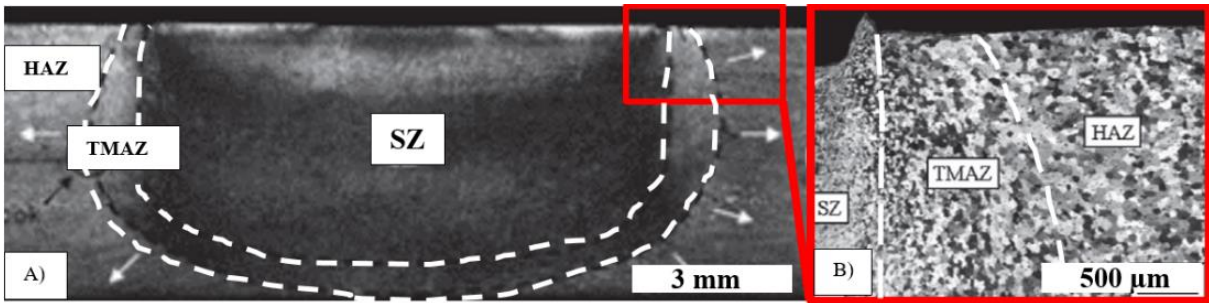
Figure 6 – Illustration of A) macrography of the cross section of the weld's button and B) transition region. Source: adapted from Suhuddin et al. (2013).

There´s no conclusive evidence in which parameter is the most significant or influent for RFSSW. The factors that have influence on the process could be consider as many as possible, although the research would not become reasonable. In order to reduce the complexity of the evaluation process, only two or three parameters are usually tested in the optimization study for the RFSSW process. For example, the study of process optimization of dissimilar RFSSW welds by Plaine et al. (2016), dwell time and tool rotation speed were investigated as two independent variables. The rotation speed is reported as the most significant parameter for LSS on the joint, followed by its interaction with dwell time. Furthermore, the HI depends on the parameters combination and increase or decrease it too much can also affect the bonding quality.

Suhuddin et al. (2013) affirmed that the plunge depth of the tool should not cross the interface between the dissimilar materials. The main reason is to avoid excessive formation of IMC, which is often formed during dissimilar welds. This compound is detrimental for the mechanical properties of the joint. Concerning the microstructure, Shen et al. (2017) presented that defects associated to the material flow reduce the LSS. In addition, preferable mechanical properties could be obtained at lower RS [Tier, 2013].

There are two types of mechanisms that can describe the failure mode: interfacial fracture and plug pullout. The former is typically associated to catastrophic brittle failure, while the latter is associated with ductile failure [Amancio-Filho, 2011].

3.3. DESIGN OF EXPERIMENTS (DOE)

The most traditional approach to understand the relationship between the process inputs and the final product is one factor at a time (OFAT) and it consists of a large number of tests and is often inefficient [Antony, 2014].

Concerning to overcome these drawbacks while ensuring the reliability of the results, it is crucial to apply statistical methods throughout the planning, execution, and analysis phases of the experimental procedure. Box-Behnken design of experiments (BBD) is a methodology based on the response of surface (RSM) to develop, test and optimize the object of study. This methodology is a subcategory from the design of experiments (DOE), which combines a mathematical model with the procedure of testing. The goal of utilizing the DOE is to assess the output performance by changing the input parameters of the process systematically. Therefore, it is a cost-effective approach, because it can provide a substantial volume of information while only a restricted set of experiments is necessary.

Analysis of variance (ANOVA) is a statistical analysis tool used to represent the significance observed in a particular factor of the experiment. Statistical analysis and experimental procedures are usually closely related. Minitab is a statistical analysis software that can apply the BBD to generate the combination of the factors and the order of experiments necessary to analyze the influence of the parameters on the interested response or final product.

4. MATERIALS AND METHODS

4.1 BASE MATERIALS

The base materials used in this study are typically employed in structural components for the automotive industry and were suggested by the Stir4Steel Project as a solution for welding dissimilar materials. The steel and aluminum plates were provided by ArcelorMittal and handled by Helmholtz-Zentrum Hereon's workshop. It was necessary to analyze dimensional requirements, mechanical properties and chemical composition to verify the reliability of the shipping.

4.1.1. AlSi-Coated Press Hardened Steel 1500 MPa (PHS1500AlSi)

The PHS1500AlSi 1.4 mm thick plate consists of a fully martensite microstructure, shown in Figure 7 A). The coating on the steel surface, for corrosion and mechanical abrasion protection, is comprised of an 18.5 µm thick eutectic AlSi layer and a 9.5 µm thick ununiform intermetallic compound layer. The second is identified by an Al_7Fe_2Si of 8.5 µm thick layer closer to the eutectic AlSi layer and an $Al_5Fe_2(Si)$ of 1.0 µm thick closer to the steel base material [Ding, 2017], as shown in Figure 7 B). The chemical composition and mechanical properties of the steel are presented in Table 1 and 2, respectively.
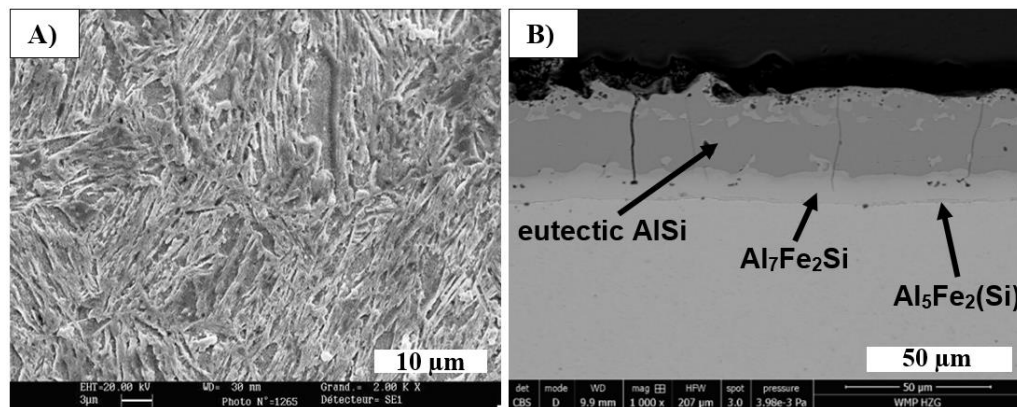
Figure 7 – SEM images from A) martensite microstructure on steel´s base material and B) AlSi-coating showing the internal layers (eutectic AlSi of 18,5 µm, Al_7Fe_2Si of 8.5 µm and $Al_5Fe_2(Si)$ of 1.0 µm). Source: A) ArcelorMittal and B) the author.

Table 1 – PHS1500AlSi chemical composition [wt%]. Source: ArcelorMittal.

	Fe	C	Si	Mn	P	S	Al	Ti	Nb	Cu	Cr
PHS 1500	97.25	0.25	0.40	1.4	0.03	0.01	0.05	0.05	0.01	0.2	0.35
AlSi-coating	0.2	-	12.5	-	-	-	87.3	-	-	-	-

Table 2 – PHS1500AlSi mechanical properties. Source: ArcelorMittal.

	Young´s Modulus	Poisson´s Ratio	Tensile Strength	Yield Stress	Elongation	Density
PHS1500AlSi	205 GPa	0.30	1500 MPa	1050 MPa	11 %	7860 kg/m³

Preliminary tests proved that it was not possible to weld the cast AlSi10 directly on the AlSi-coating, contradicting the results from Ding et al. (2017) and Shen et al. (2019) despite the materials and procedures being different.

In order to guarantee the bonding of the weld, it was necessary to test the steel plates in three superficial conditions: original AlSi-coating, internal Al_7Fe_2Si IMC and completely removed coating layer of the PHS plates. These surface conditions have the agreement of the

S4S partners and were defined as it follows:

     a) Original AlSi-coating: rinsed the surface with industrial ethanol 99% and dried naturally;

     b) Internal Al_7Fe_2Si IMC layer: eutectic AlSi was chemically removed with an aqueous NaOH saturated solution to reach the second IMC layer, polished the IMC surface with an angular grinder with polishing cloth and rinsed the surface with industrial ethanol 99% and dried naturally;

     c) Uncoated steel plate: removed the AlSi-coating completely to reach the steel surface with an angular grinder with sanding paper #200, polished the steel surface with an angular grinder with polishing cloth and rinsed the surface with industrial ethanol 99% and dried naturally.

4.1.2. Die Cast Aluminum (AlSi10)

The AlSi10 3.0 mm thick plate features primary dendrites of Al into the matrix of eutectic AlSi. The microstructural feature is independent of the material thickness position and there are some casting defects such as internal voids, shown in Figure 8. The chemical composition and mechanical properties of the AlSi10 are presented in Table 3 and 4, respectively.
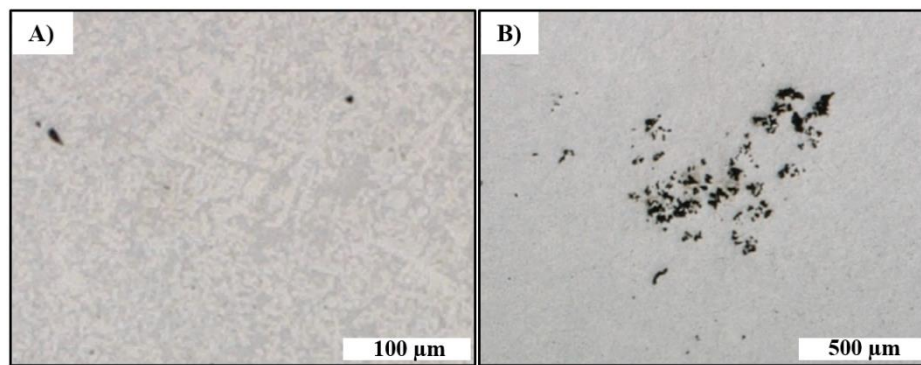

Figure 8 – Optical microscope image showing A) primary dendrites of Al into the matrix of eutectic AlSi and B) casting defects such as internal voids. Source: the author.

Table 3 – AlSi10 chemical composition [wt%]. Source: ArcelorMittal.

	Al	Si	Mg	Mn	Fe	Cu	Ti	Sr	Impurities
Cast AlSi10	88.62	10.00	0.30	0.60	0.22	0.10	0.05	0.01	0.15

Table 4 – AlSi10 mechanical properties. Source: ArcelorMittal.

	Young´s Modulus	Poisson´s Ratio	Tensile Strength	Yield Stress	Elongation	Density
Cast AlSi10	75 GPa	0.33	200 MPa	120 MPa	18 %	2600 kg/m^3

Due to the insufficient quality of a few coupons of AlSi10 3.0 mm thick plates, every coupon was scanned by X-ray micro-CT scan to assess the internal quality, Figure 9. The welding region should be completely free of defects, as shown in Figure 9 B). The bad quality plates, Figure 9 A), were discarded computing approximately 5 % of the total amount.
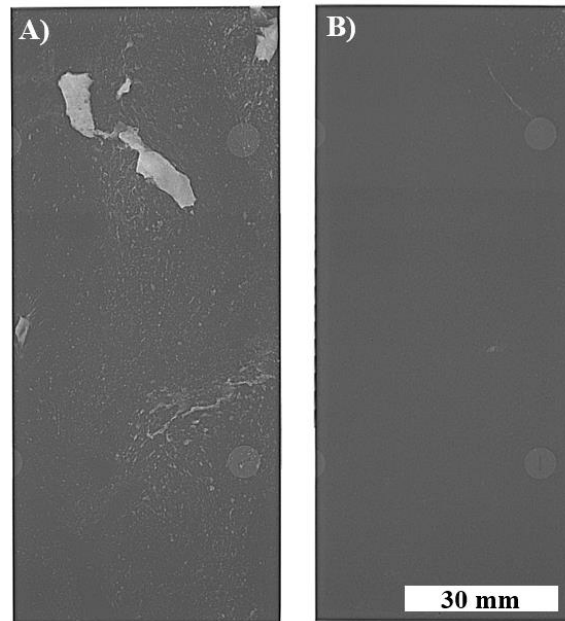
Figure 9 – X-ray micro-CT scan presenting A) insufficient quality plate with internal voids and B) standard quality plate. Source: the author.

4.2. WELDING MACHINE AND TOOL

The welding machine used in this study is the Harms&Wende RPS100-V32. The clamping force, axial load, tool position, welding time and rotational speed were acquired and recorded by internal sensors. However, temperature and torque were not taken into account. The axial position of the tool can be set with an accuracy of 0.01 mm. According to different welding processes, a variety of sizes and materials for the welding tool can be used on the machine. In this study, a non-consumable welding tool made from M4 high-speed steel (ASTM A600) was chosen. The three pieces tool set has a probe of 6 mm, a shoulder of 9 mm and a clamping ring of 17 mm. Figure 10 illustrates the machine and the tool set.
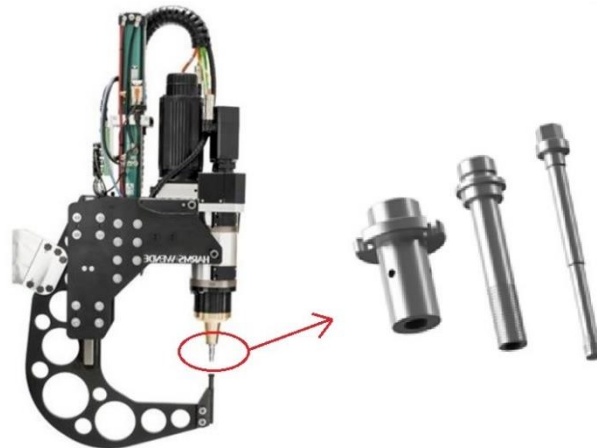
Figure 10 – Schematic illustration of the RPS100-V32 welding machine and exploded view of the welding tool. Source: Harms&Wende.

For the shoulder plunge welding mode, the travel factor (TF) defines the relation between the plunging displacement of the shoulder and the retraction displacement of the probe to ensure the plasticized material will not be over or under-compressed during the refill stage. The travel factor can be calculated using volumetric relations. According to the tool dimensions used in this study, the travel factor is 0.8.

4.3. WELDING PROCEDURES

This work was carried out at WMP Department at Helmholz-Zentrum Hereon in Geesthacht, Germany. A welding procedure was developed, in order to guarantee consistent results with reproducibility based on standard ISO 18785:2018, standard ISO 14273:2016 and previous works [Fisher, 2015; Santos, 2020; Shen, 2022].

The sample sizing of the test was in accordance with ISO 14273:2016 for saturated lap shear strength condition. This standard was adopted because of the inexistence of any standard about samples sizing for this friction-based process. For this reason, the plates were cut to rectangular coupons of 115 mm long by 50 mm wide. The overlap area was 45 mm long by 50 mm wide, where the spot weld was located at the geometric center of it, as shown in Figure 11.

Figure 11 – Schematic illustration of the assembling of test coupons and sample sizing for saturated condition of LSS test. Source: adapted from ISO 14273:2016.

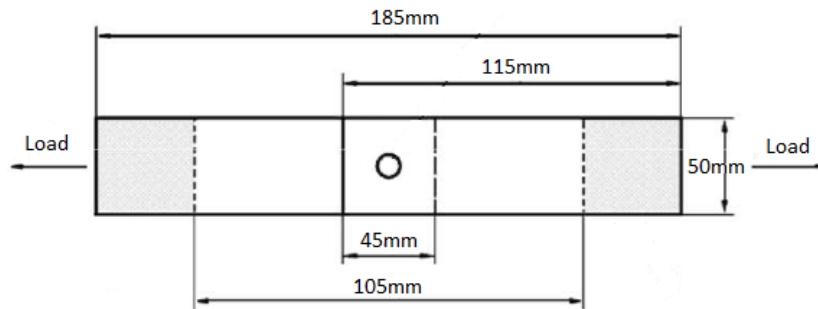The welding coupons were cleaned with industrial ethanol to remove impurities and to degrease the surface. Before each welding batch to obtain the results for this work, preliminary weldings were produced to preset the zero leveling, heating the tool and filling the clearance between the small gaps of the tool-set. After a few welds, the surface quality should be smooth and steady. The quantity of test plates depends on the quality obtained on the preliminary weldings.

The three mean welding parameters chosen for this study, based on preliminary tests and previous works [Suhuddin, 2013; Plaine, 2016; Shen, 2017], were RS, PS and DT. The parameters defined as fixed were CF = 12 kN and PD = 2.9 mm, also based on the best results from preliminary experiments.

4.3.1. Defect-free Process Parameters Window

The first step to achieve the process optimization results was the parameters combination selection, the wider as possible to produce defect-free welds (RS from 1000 rpm to 3000 rpm, PS from 0.5 mm/s to 1.5 mm/s and DT from 0 s to 2 s). This means that preliminary tests were performed to find the maximum and minimum levels for the mean welding factors aiming to produce sound joints. These tests were also important to understand the bonding mechanism and even if the dissimilar material combination was possible to produce. The RPS100-V32 machine parameters range was not exceeded to guarantee the equipment and the tool set longevity.

The criteria for considering a defect-free weld, for this study, was based on satisfactory results from the three analysis methods: 3D profilometer, optical microscope and LSS performance. Satisfactory results considered, at the same time, the absence of annular grooves, lack of filling and internal voids on the SZ of the weld. Regarding the LSS, the minimum requirement for shear load was 4.56 kN and the minimum on average was 5.72 kN, based on the standard AWS D17-2:2007.

4.3.2. Design of Experiments (DOE)

The optimization of process parameters in terms of the mechanical performance was conducted with Box-Behnken design of experiments. With the support of the statistical analysis software Minitab, the combination of the factors could be generated. The experiment considered the sequence of 15 combinations and they were performed in triplicate and in random order producing 45 welds in total. After producing the batch of welds, they were tested for LSS.

The experimental responses are evaluated to fit a mathematical model. Considering a confidence level of 95 %, the significance of each model can be determined by the corresponding p-value in the ANOVA table and trough Pareto's chart.

Minitab was used to predict the best combination of parameters that were responsible for achieving maximized LSS welds with minimum deviation, not necessarily tested in the experiment. A sequence of six welds, with the optimized parameters combination, was performed to confirm this prediction. Three welds were tested for LSS and the other three were assessed with 3D profilometer and optical microscope to confirm the inexistence of defects.

4.4. ANALYSIS PROCEDURES

4.4.1. 3D Optical Profilometer

In order to evaluate the quality of the surface of the weld´s nugget, the Keyence 3D Optical Profilometer VR-6000 was adopted to measure the topography of the weld's button surface. This method can evaluate the annular groove and lack of filling or mixing. The following procedure could ensure the same conditions for assessment from the testing samples until the optimized ones. The magnification mode utilized for 17 mm diameter welds was 40x with high magnification lenses, the area of mapping was defined by 19 mm x 19 mm and the auto-focus was settled always on the lower region of the weld´s button.

4.4.2. Metallographic Preparation

The samples for metallographic analysis were prepared by sectioning them at a 2 mm away from the weld's centerline by a Struers Secotom-50 using a 50A20 disc at 2500 rpm rotation speed and 0.25 mm/s linear displacement rate. Each sample was identified with a printed label and embedded with Demotec-20. The resin was cured inside a pressure pot with 2 bar of pressure for 20 minutes to prevent bubbles and opacity.

Once mounted, the samples were ground and polished using a Struers Tegramin grinding and polishing machine. The grinding procedure started from SiC paper #80 to #4000 and polishing from 9 µm until 1 µm. Finally, the surface was cleaned with industrial ethanol 99%. However, the samples were not etched, because the defect investigation was already visible in the microscope.

4.4.3. Optical Microscope

The cross section of the welds and defects were evaluated using a Keyence VHX-6000 digital microscope. The cross-sectional images of the joint were generated under magnification of 50x to 150x, depending on the quality of the stitching picture. The light mode used was fully axial with an auto-white feature. The images included the complete area of the perpendicular cross section of the plates (SZ, TMAZ, HAZ and BM).

4.4.4. Lap Shear Strength (LSS)

The mechanical properties of the joints were evaluated through quasi-static lap shear

tests with a Zwick/Roell universal tensile testing machine for a 250 kN maximum load. The displacement, in mm, and the load, in kN, measurements were obtained and controlled using TestXpert software at a constant shear rate of 1 mm/min.

The test specimen dimensions, as specified before, are larger than normal tensile test specimen sizes. The reason is to achieve the maximum measurement of the strength of the welds in the saturated strength condition. According to standard ISO 14273:2016, this condition is obtained when the coupon´s dimensions are wider and longer enough, preventing secondary bend.

5. RESULTS AND DISCUSSION

In order to study the feasibility of joining dissimilar materials by RFSSW, achieve the defect-free process window, optimize the main response of LSS and understand the influence of the welding parameters, several statistical procedures and welding tests have been produced. A representative surface of an overlapped AlSi10 3.0 mm thick plate welded to a PHS1500AlSi 1.4 mm thick plate by RFSSW is shown in Figure 12, highlighting the good surface finish of the weld button.

Figure 12 – A representative surface of overlapped AlSi10 welded to a PHS1500AlSi by RFSSW, highlighting the good surface finish. Source: the author.

5.1 DEFECT-FREE PROCESS PARAMETERS WINDOW

Preliminary tests were carried out to evaluate and understand the bonding behavior between the dissimilar materials through the AlSi-coating. Figure 13 shows that the original AlSi-coating does not have sufficient mechanical strength to withstand shear loads or to hold the plates together.
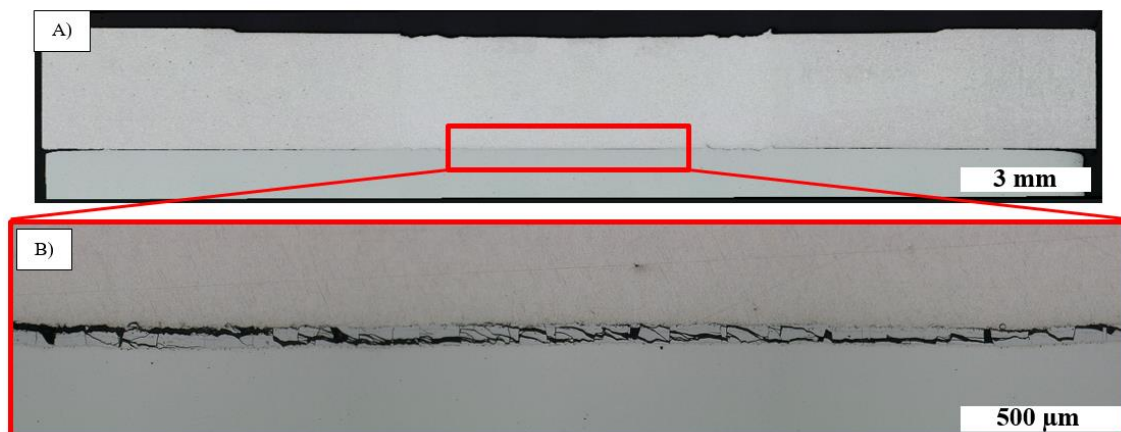

Figure 13 – Optical microscope image from a preliminary weld to assess the bonding behavior through the original AlSi-coating showing A) the cross section of the weld and B) the interface with no bonding. Source: the author.

From this fact, two more coating conditions were tested: exposed internal Al$_7$Fe$_2$Si IMC and completely removed coating layer from the PHS plates. The following parameter combinations, presented in Table 5, were welded to evaluate the joinability for both conditions. The optical microscope assessed the bonding interface and internal defects, while the 3D profilometer, the weld´s surface quality.

Table 5 - Preliminary tests to evaluate the joinability for both conditions.

Parameter	RS [rpm]	PS [mm/s]	DT [s]	Al$_7$Fe$_2$Si IMC	Uncoated
ET_04	2500	1.00	1.0	ok	ok
ET_05	1500	0.75	1.0	ok	ok
ET_08	1500	2.00	1.0	ok	ok
ET_09	1500	1.00	0.0	ok	ok
ET_13	1500	1.00	2.0	ok	ok
ET_14	2500	0.75	1.0	ok	ok
ET_15	2500	0.50	0.5	ok	ok
ET_16	2500	0.50	1.0	ok	ok
ET_17	2500	1.50	2.0	ok	ok
ET_18	1000	1.00	0.0	unsatisfactory	unsatisfactory
ET_19	1000	1.50	0.0	unsatisfactory	unsatisfactory
ET_20	1000	2.00	0.0	unsatisfactory	unsatisfactory

Results from the preliminary tests, as cross-sectional images from an optical microscope and superficial quality from a 3D profilometer, proved that both conditions were weldable for every tested parameter combination. However, unsatisfactory results were also obtained, pointing that lower HI increased the load level for the machine's rotor and for the tool. Lower RS produced internal voids, due to insufficient stirring and mixing of material. Then, 1500 rpm should be the lowest RS for further testing. For the same reason, PS should not be over 1.5 mm/s.

The following parameter combinations were tested for LSS for both coating conditions, in order to evaluate the mechanical performance, presented in Table 6. The difference of LSS values between the two coating conditions was given in terms of uncoated LLS minus IMC LSS, in kN.

Table 6 - Preliminary tests to assess the LSS for both steel surface conditions.

Parameter	RS [rpm]	PS [mm/s]	DT [s]	Al$_7$Fe$_2$Si IMC LSS [kN]	Uncoated LSS [kN]	Difference [kN]
ET_09	1500	1.00	0.0	6.87	8.09	+1.22
ET_14	2500	0.75	1.0	7.20	8.49	+1.29
ET_15	2500	0.50	0.5	7.98	8.35	+0.37
ET_16	2500	0.50	1.0	7.49	8.20	+0.71
ET_17	2500	0.50	2.0	7.52	8.63	+1.11
ET_21	1500	1.50	0.0	7.96	6.35	-1.61
ET_22	1500	1.50	2.0	7.81	8.81	+1.00
ET_23	2000	1.00	2.0	8.11	8.38	+0.27

The results from all the analysis concluded that the original AlSi-coating was unfeasible to weld with cast AlSi10. The exposed Al$_7$Fe$_2$Si IMC layer could achieve good results with cast AlSi10, about 7.60 kN in average LSS, presenting 33.21 % more LSS than the minimum required from the standard AWS D17-2. Finally, the uncoated steel was the best option, with about 8.20 kN in average LSS, presenting 42.65 % more LSS than the minimum required from standard and approximately 0.55 kN greater than the exposed IMC condition. From these facts, the uncoated steel was adopted to proceed with the process optimization tests.

In order to optimize the process of welding dissimilar materials by RFSSW, the limits of the parameter combination window that would result in defect-free welds were found, based on the presented tests and results, as shown in Table 7.

Table 7 - Defect-free parameter combination window.

	Lower Limit	Medium Value	Upper Limit
RS [rpm]	1500	2000	2500
PS [mm/s]	0.5	1.0	1.5
DT [s]	0	1	2

5.2 PROCESS PARAMETERS OPTIMIZATION (DOE)

Box-Behnken design of experiments was applied for process parameters optimization to deliver maximized LSS welds with minimized standard deviation. The statistical analysis software Minitab generated, from the achieved defect-free process parameters window, 13 different combinations of factors. The central point of the cube from BBD was triplicated, computing 15 combinations. The weldings were performed in triplicate and in random order, producing 45 welds in total.

Table 8 presents the parameter combination in ascending levels order of the factors with the related LSS results. The results from mechanical testing of LSS were satisfying enough, bringing the average value close to 8.0 kN. Three outlier values were obtained and could occur due to external variables from the material quality or processing errors. Those values did not affect the optimization result, as Box-Behnken already predicted these events.

Table 8 - Process parameters combination from Box-Behnken design with the results of LSS testings.

RS [rpm]	PS [mm/s]	DT [s]	LSS 1 [kN]	LSS 2 [kN]	LSS 3 [kN]
1500	1.0	0	6.22	7.83	2.98
1500	0.5	1	8.33	8.42	9.03
1500	1.5	1	7.49	7.48	7.82
1500	1.0	2	8.69	8.34	5.98
2000	0.5	0	6.87	7.88	8.51
2000	1.5	0	7.66	7.80	8.05
2000	1.0	1	8.10	8.04	6.05
2000	1.0	1	8.31	8.39	8.22
2000	1.0	1	8.41	8.61	8.36
2000	0.5	2	8.19	7.75	8.66
2000	1.5	2	7.66	8.28	8.13
2500	1.0	0	7.11	7.53	7.73
2500	0.5	1	8.49	8.41	8.38
2500	1.5	1	7.48	7.53	6.91
2500	1.0	2	8.30	8.35	8.55

To assess the data, the Pareto's chart was employed to identify the main parameters and interaction that contribute the most to the process, as shown in Figure 14. From this results, there was no factor or combination of factors that were responsible for the variability in LSS, with confidence level over 95%. Overall, this result indicates that the model did not have a good correlation, although the DT has a much higher sensitivity to LSS in comparison with PS and RS.
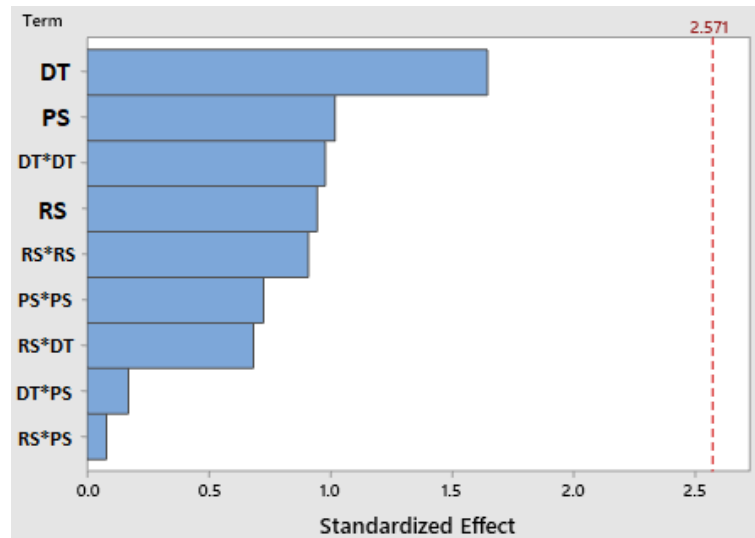
Figure 14 – Pareto chart analysis of the main parameters and interactions for LSS. Source: the author.

Minitab uses a full quadratic model to fit the response of the LSS results from Box-Behnken design for the ANOVA, presented in Table 9. The p-value is calculated using degrees of freedom (DF), adjusted sums of squares (Adj SS), adjusted mean squares (Adj MS), and f-value for each term. The results clearly demonstrated a model with a p-value of 0.614, which means that the model fails to explain variation in LSS with a 95 % of confidence level. This conclusion also matches the previous result from Pareto's chart. The result can be attributed to the three outlier values that occurred in the experimental data.

Table 9 – ANOVA for LSS results from BBD.

Source	DF	Adj SS	Adj MS	F-Value	P-Value
Model	9	4.442	0.493	0.84	0.614
Linear	3	2.730	0.910	1.55	0.311
RS	1	0.527	0.527	0.90	0.387
DT	1	1.593	1.593	2.71	0.160
PS	1	0.610	0.610	1.04	0.355
Square	3	1.415	0.471	0.80	0.543
RS^2	1	0.486	0.486	0.83	0.404
DT^2	1	0.563	0.563	0.96	0.372
PS^2	1	0.309	0.309	0.53	0.500
Interaction	3	0.296	0.098	0.17	0.913
RS*DT	1	0.275	0.275	0.47	0.524
RS*PS	1	0.003	0,003	0.01	0.939
PS*DT	1	0.016	0.016	0.03	0.872
Error	5	2.935	0.587	-	-
Lack of fit	3	2.275	0.758	2.30	0.318
Pure error	2	0.660	0.330	-	-
Total	14	7.377	-	-	-

For this study, Minitab was used to analyse the individual influence of the factors and the interaction between the factors as well, through analysis of variance. Table 10 presents the prediction of the software. These values are reasonable considering the batch of testings from Table 8 and comparing it to the levels of the parameters. Equation 1 presents the regression equation in uncoded units for desirability of LSS response and Figure 15 shows graphically the results.

Table 10 – Optimized process parameters combination with the prediction of LSS.

	RS [rpm]	PS [mm/s]	DT [s]	Prediction
Optimized combination	2200	0.5	1.5	8.67 kN

$$LSS \ = \ 0.67 + 6.79 \ 10^{-3} \ RS + 2.41 \ DT - 2.59 \ PS - 10^{-6} \ RS^2$$
$$-3.91 \ 10^{-1} \ DT^2 + 1.16 \ PS^2 - 5.25 \ 10^{-4} \ RS \ DT$$
$$-1.2 \ 10^{-4} \ RS \ PS - 1.3 \ 10^{-1} \ DT \ PS \qquad \text{Equation 1}$$
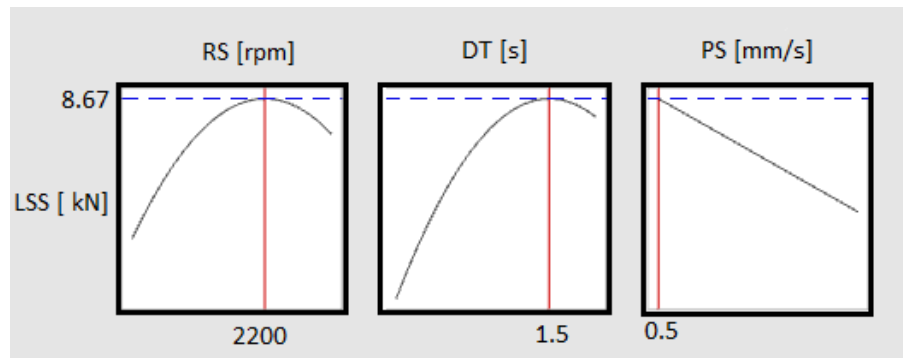

Figure 15 – Graphic representations of the influence of each parameter on LSS. Source: the author.

Comparing this optimized combination to the defect-free window, the RS and DT values were relatively high and the PS value was the lowest. These results are cognate with previous studies of dissimilar RFSSW weldings [Peng, 2020].

Since the optimized parameter is a new combination that was not included in the Box-Behnken experimental design, the prediction of Minitab was tested. Three welded samples were produced to assess the surface quality by the 3D profilometer and cross-sectional features by the optical microscope, presented in Table 11. Table A.1 and A.2, in Appendix A, present those results in detail. In addition, three more welded samples were produced for mechanical performance testings, presented in Table 12.

Table 11 – Optimized process parameters combination welds with the results of the 3D profilometer and optical microscope analysis.

	3D Profilometer	Optical Microscope
E_op_1	ok	ok
E_op_2	ok	ok
E_op_3	ok	ok

Table 12 – Optimized process parameters combination with the results of the LSS testings.

	LSS 1	LSS 2	LSS 3	LSS average	LSS deviation
Optimized combination	8.13 kN	8.31 kN	8.19 kN	8.21 kN	0.075 kN

The predicted LSS value from Minitab was 0.46 kN higher than the actual optimized value. This means an error of 5.30 %, which is a reliable result. In addition, the lower deviation for LSS tests, about 0.91 %, guarantees a consistent process with reproducibility.

6. CONCLUSIONS

The present study optimized the process parameters combination of refill friction stir spot welding for the response of LSS between cast aluminum (AlSi10) 3.0 mm thick plates and press hardened steel (PHS1500AlSi) 1.4 mm thick plates in the configuration of overlapped sheets.

During the tests and experiments, it was possible to find the parameter combination window that would result in defect-free welds. In addition, the feasibility of welding three different surface conditions of the PHS1500AlSi were attempted. The uncoated surface of the steel was the best option to continue with the process parameters optimization.

Box-Behnken design of experiments was used to carry out multiple response surface methodology for optimization of process parameters. Furthermore, the analysis of variance was used to assess the significance of each parameter for the LSS test response. Minitab statistical software was used to predict the parameters combination (RS = 2200 rpm, DT = 1.5 s, PS = 0.5 mm/s) that achieved maximized results for LSS with minimized standard deviation. The regression equation in uncoded units and visual graphs for LSS were demonstrated. The RS and DT values were relatively high and the PS, the lower.

7. FUTURE WORKS

The uncoated condition of the steel plate opens the possibility to continue some studies for corrosion mechanisms. For future works, the process parameters optimization using adhesive sealant should be considered. In addition, the fatigue life behavior of dissimilar joints, the design optimization of multi-spots and other combinations of steels and Al alloys should be investigated.

8. REFERENCES

Amancio-Filho, S. T.; Camillo, A. P. C.; Bergmann, L.; dos Santos, J. F.; Alcântara, N.G. **Preliminary investigation of the microstructure and mechanical behaviour of 2024 aluminium alloy friction spot welds**. Materials Transitions. pp 52. 2011.

Antony J. **Design of experiments for engineers and scientists**. 2014.

ArcelorMittal. **Steel and Aluminum datasheet for automotive industries**. Disponível em: https://automotive.arcelormittal.com/products. Acesso em: Outubro de 2023.

AWS D17.2/D17.2M:2007 – **Specification for Resistance Welding for Aerospace Applications.**

Costa, S. A. L. V., Mei, P. R. **Aços e Ligas Especiais**. São Paulo: Edgard Blacher. 2a Ed. 646p. 2006.

Cao, J.Y., Wang, M. **Microstructure, texture and mechanical properties during refill friction stir spot welding of 6061-T6 alloy.** Materials Characterization, 2016.

Ding, Y., Shen, Z., Gerlich, A. P. **Refill friction stir spot welding of dissimilar aluminum alloy and AlSi-coated steel**. Journal of Manufacturing Process. Vol 30, pp 353-360. 2017.

Fisher, V. F. S. **Aplicação do Processo de Soldagem a Ponto por Fricção (FSpW) Entre Juntas Dissimilares de Aço e Liga de Alumínio para Aplicações Automotivas**. 2015. Dissertação (Programa de Pós-Graduação em Engenharia de Minas, Metalúrgia e de Materiais PPGE3M) Universidade Federal do Rio Grande do Sul, Porto Alegre, 2015.

Hartlieb, M. **Aluminum alloys for structural die-casting**. Die Casting Eng. (3) 40–43. 2013.

ISO 14273:2016 – **Specimen Dimensions and Procedure for Tensile Shear Testing Resistance Spot Welds.**

ISO 18785:2018 – **Friction Stir Spot Welding – Aluminum.**

Mitra, T. K. **Welding of Aluminum Alloys.** Welding Research Institute Journal, Vol. 22. pp. 22-30. 2001.

Nandan, R. **Recent Advances in Friction Stir Welding – Process, Weldment Structure and Properties.** Prog Mater Sci 53 (6): 980 – 1023, 2008.

Peng, L. Chen, S., Dong, H., Hua, J., Yang, G. **Interfacial microstructure and mechanical properties of dissimilar aluminum/steel joint fabricated via refilled friction stir spot weldings.** Journal of Manufacturing Processes. Vol. 49: 385-396. 2020.

Plaine, A. H., Gonzalez A. R., Suhuddin, U. F. H., dos Santos, J. F. **The optimization of friction spot welding process parameters in AA6181-T4 and Ti6Al4V dissimilar joints.** Materials & Design, vol. 83, pp. 36-41, 2016.

dos Santos J.F., Schilling C., inventors; Helmholtz-Zentrum GZ, assignee. **Method and device for linking at least two adjoining work pieces by friction welding**. US patent 6722556B2. 18 Nov. 1999.

Santos, P. M. S. **Development of refill friction stir spot welding (RFSSW) for lightweight welding applications**. PhD Thesis. Coventry University, 2020.

Shakil S. I., **Additive manufactured versus cast AlSi10Mg alloy: Microstructure and micromechanics**. Results in Materials, Vol 10:100178. June 2021.

Shen, J., Lage, S. B. M., Suhuddin, U., dos Santos J. F. **Texture Development and Material Flow Behavior During Refill Friction Stir Spot Welding of AlMgSc**. Metallurgical and Materials Transactions. Vol. 49, pp. 241-254, 2017.

Shen, T. **Mechanical Properties and Microstructures of Refill Friction Stir Spot Welded Aluminum Alloy 2219 Joints**. 2022. MSc Thesis. Aachen University, Hamburg, 2022.

Shen, Z., Ding, Y., Chen, J. **Interfacial bonding mechanism in Al/coated steel dissimilar refillfriction stir spot welds.** Journal of Materials Science and Technology. Vol 35, pp 1027-1038. 2019.

Stir4Steel Project. **Helmholtz-Zentrum Hereon: Stir4Steel Project.** 2021. Disponível em: https://hereon.de/about_us/eu_projects/h2020/key/103753/index.php.en. Acesso em: Outubro de 2023.

Suhuddin, U.; Campanelli, L.; Bissolatti, M.; Wang, H.; Verastegui, R.; dos Santos, J.F. **A review on microstructural and mechanical properties of friction spot welds in Al-based similar and dissimilar joints**. Woodhead Publishing, pp. 15–21. Symp. Join. Weld, 2013.

Thomas W. M. E. D. N. **Friction stir butt welding**. Patent GB. Patent 9125978.8, 1991.

Tier, M., Rosendo, T., dos Santos J. F., Huber, N., Mazzaferro, J. A., Mazzaferro, C. P., Strohaecker T.R. **The influence of refill FSSW parameters on the microstructure and shear strength of 5042 aluminum welds**. J Mater Process Technol; 213: 997–1005. 2013.

Wang, K. K, Lin W. **Flywheel Friction Stir Welding Research**. AWS. June 1974

World Steel Association. Disponível em: https://worldsteel.org/about-steel/about-steel. Acessado em: Julho de 2023.

Yang, X. W., Fu, T., Li, W. Y., **Friction Stir Spot Welding: A Review on joint macro-and microstructure, property, and process modelling**. Advances in Materials Science and Engineering, p. 11, 2014.

Zou, Y., Li, W., Xu, Y., Shen, Z. **Detailed characterizations of microstructure evolution, corrosion behavior and mechanical properties of refill friction stir spot welded 2219 aluminum alloy.** Materials Characterization, 2021.

APPENDIX A – OPTIMIZED PROCESS PARAMETERS RESULTS

Table A.1 – Welds performed with optimized process parameters combination showing the results of 3D profilometer analysis. Source: the author.
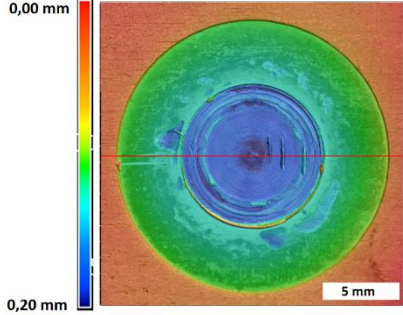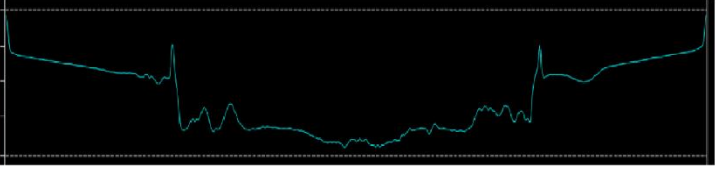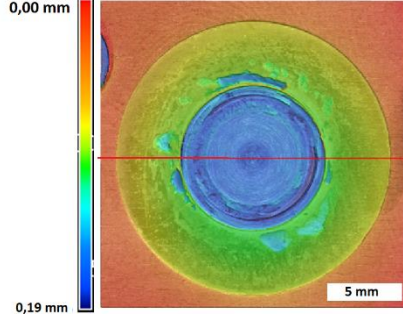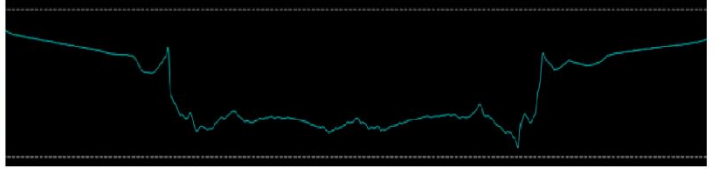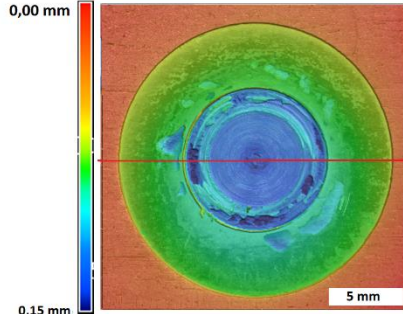
	3D Profilometer
E_op_1	
E_op_2	
E_op_3	

Table A.2 – Welds performed with optimized process parameters combination showing the results of optical microscope analysis. Source: the author.

	Optical Microscope
E_op_1	
E_op_2	
E_op_3	